Value of contrast-enhanced ultrasound for detection of synovial vascularity in experimental rheumatoid arthritis: an exploratory study

Hui Liu[1], Chao Huang[2,*], Shuqiang Chen[1,*], Qing Zheng[3], Yuhong Ye[4], Zhen Ye[1] and Guorong Lv[5,6] (iD)

Abstract

Objective: This study aimed to examine the associations between contrast-enhanced ultrasound (CEUS) imaging and synovial hypervascularity and synovitis score in a rabbit model of antigen-induced arthritis (AIA), compared with power Doppler ultrasound (PDUS).

Methods: We investigated 50 knee joints in 25 AIA rabbits (AIA group), and 10 knee joints in five sham-injected rabbits (control group). PDUS and CEUS images were evaluated at the 8th week. Ultrasound-guided synovial biopsies were targeted in the area with hypervascularity, and synovial microvessel density (MVD) was evaluated by immunohistochemical staining of CD31.

Results: The PDUS score was significantly higher in the AIA group (2.61 ± 0.78) compared with the control group (0.50 ± 0.53). CEUS in the AIA group revealed a fast-in/slow-out pattern of contrast enhancement. MVD revealed by CD31+ vessel count and the synovitis score were significantly higher in the AIA group compared with the control group. In the AIA group, CEUS findings showed a better correlation with MVD revealed by CD31+ and synovitis score than PDUS findings.

Conclusion: CEUS is superior to PDUS for estimating synovial hypervascularity and hyperplasia in experimental rheumatoid arthritis.

[1]Department of Ultrasound, the First Affiliated Hospital of Fujian Medical University, Fuzhou, China
[2]Department of Nuclear Medicine, the First Affiliated Hospital of Fujian Medical University, Fuzhou, China
[3]Department of Hematology and Rheumatology, the First Affiliated Hospital of Fujian Medical University, Fuzhou, China
[4]Department of Pathology, the First Affiliated Hospital of Fujian Medical University, Fuzhou, China

[5]Department of Ultrasound, the Second Affiliated Hospital of Fujian Medical University, Quanzhou, China
[6]Department of Clinical Medicine, Quanzhou Medical College, Quanzhou, China

*These authors contributed equally to this work.

Corresponding author:
Guorong Lv, Department of Ultrasound, the Second Affiliated Hospital of Fujian Medical University, 34 Zhongshan North Rd, 362000 Quanzhou, China.
Email: lgr_feus@sina.com

Introduction

Rheumatoid arthritis (RA) is characterized by synovial inflammation and hyperplasia, autoantibody production, cartilage and bone destruction, and systemic features including cardiovascular, pulmonary, psychological, and skeletal disorders.[1] A therapeutic revolution in the treatment of RA over the past decade has transformed articular and systemic outcomes,[2] and remission can be achieved if the disease is identified early and treated promptly and continuously.[3] However, some individuals fail to respond adequately to treatment and sustained remission is rarely achieved.[1,3]

The development and proliferation of pannus is a crucial event in the pathogenesis of RA, and can be seen before the destruction of the cartilage and bone.[4] Pannus vascularization may be a key event in the invasive and destructive behavior of RA.[5,6] Neoangiogenesis is a characteristic feature of early and established synovitis, and an early and crucial event promoting the development of the hyperplasic proliferative pathologic synovium.[7,8] RA is initially characterized by marked hyperplasia of macrophage-like and fibroblast-like synoviocytes in the lining layer in the prevascular stage, followed by increased capillary density in the synovium in the vascular stage, usually in the clinical phase of RA.[1,9] Although the question of whether angiogenesis drives RA or whether the enhanced synovial proliferation promotes angiogenesis remains unsolved, the available preclinical evidence suggests that anti-angiogenic treatments have a beneficial effect on RA.[9]

To achieve an early diagnosis of RA and to implement a treat-to-target (T2T) approach, the detection of abnormal synovial vascularity has the potential to be used as a screening and monitoring tool to increase the likelihood of remission and prevent structural damage.[10]

Hypervascularization of the pannus and neoangiogenesis are usually induced by inflammatory activity. However, recent studies[11–14] revealed discordant relationships between color or power Doppler imaging and the extent of inflammation and vascularity in synovial biopsies in RA patients. Although color Doppler ultrasound (CDUS) imaging allows the detection of vascularity,[15–19] its ability to detect slow flow and flow in small vessels is limited. Compared with unenhanced power Doppler ultrasound, contrast-enhanced ultrasound (CEUS) has demonstrated a better ability to characterize the vascularization in the inflamed synovium,[20] because the contrast agent[21] not only improves the detection of the color signal and the extension of vascularization,[22,23] but also allows the quantitative assessment of inflammation.[24]

Several studies have used CEUS to quantify synovial vascularity in patients with RA or psoriatic arthritis,[25–27] and it has even been used to ablate synovial pannus in antigen-induced arthritis in rabbits.[28] We previously showed that sonographic findings correlated better with histologic scoring than did serologic biomarkers of disease activity in a RA rabbit model, especially in the early stages of RA.[29] As a marker of progenitor

endothelial cells for angiogenesis,[30] CD31-positivity (CD31+) has been used to reveal the different aspects and characteristics of the tumor vasculature,[31] and several studies have revealed a significant correlation between CEUS parameters and microvessel density (MVD) indicated by CD31 immunohistochemical staining.[32–35] The goal of the current study was to examine the association between CEUS imaging and synovitis score and synovial hypervascularity in an antigen-induced arthritis (AIA) model, compared with PDUS.

Materials and methods

Antigen-induced arthritis model

Thirty male New Zealand White rabbits were randomly assigned to either the AIA (n = 25) or sham-injected control group (n = 5). The development of the AIA RA model, including basic sensitization and joint sensitization, has been described elsewhere.[29,36,37] Experimental reagents including chicken egg white albumin (A-5378) and Freund's complete adjuvant (F-5881) were obtained from Sigma-Aldrich (Burlington, MA, USA). The experimental reagents were replaced by saline in the sham-injected rabbits. The study protocol was approved by the Animal Ethics and Welfare Committee of Fujian Medical University (reference number of SYXK [min] 2016-0008) and the study was conducted in accordance with the ARRIVE (Animal Research: Reporting of In Vivo Experiments) guidelines.[38]

Unenhanced PDUS

Ultrasound imaging of bilateral knee joints was performed at the 8th week using a LOGIQ E9 machine equipped with a linear array probe, operated at a transmission frequency of 7 to 12 MHz (GE Healthcare, Waukesha, WI, USA). The procedure was carried out by a single sonographer experienced in assessing musculoskeletal disease. The rabbits were placed in a supine position and anesthetized by injection of 1% pentobarbital sodium in the ear vein at a dose of 3 mL/kg. Ultrasound parameters including acoustic gain, depth, and focus were optimized for each knee joint.

PDUS was scanned after grayscale ultrasound, to ensure acquisition of the best imaging plane. The PDUS findings of synovial blood flow were recorded using a semi-quantitative score where 0 = no PD signal, 1 = minimal PD signal, 2 = moderate PD signal, and 3 = strong PD signal[39–41] (Figure 1).

Contrast-enhanced CEUS

After standard ultrasound imaging, the bilateral knee joints were examined by real-time CEUS after injection of the intravascular tracer SonoVue (0.1 mL/kg) (Bracco SpA, Milan, Italy). Continuous scanning was started shortly before injection of the contrast agent at a rate of 15 frames per second. The operator kept the transducer stable throughout the whole process. The beam focus was placed at the level of the synovial proliferation or immediately below it, and beam gain was set at the minimum level. The left knee joint was assessed first, followed by the right knee using the same ultrasound parameters. All CEUS images were recorded as digital video images. The synovial enhancement was quantified offline independently by two investigators using the time–signal intensity curve analysis software installed on the LOGIQ E9. Highly enhanced synovial regions were manually and independently defined as the region of interest (ROI). The size of the ROI was maintained at approximately 2 to 3 mm in diameter as far as possible. The contrast-enhancement time-intensity curves were plotted based on three selected ROIs for
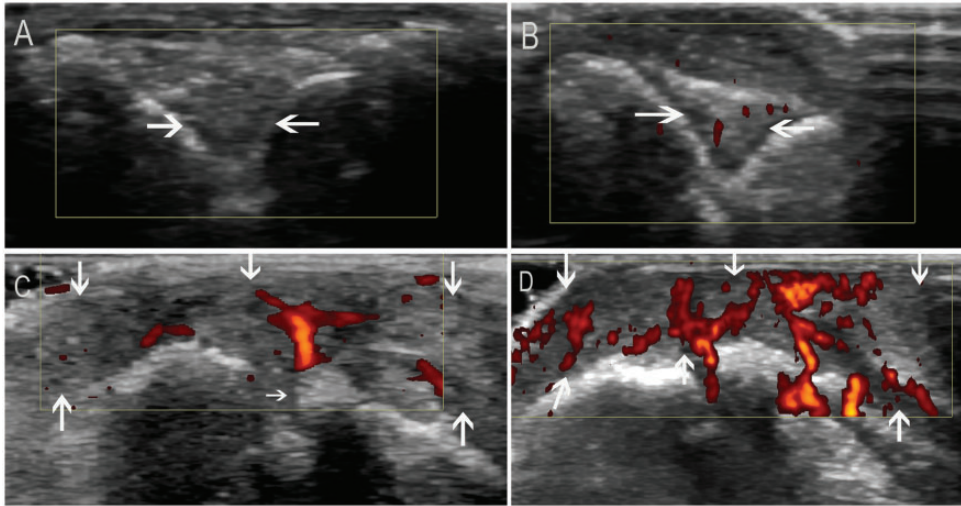
Figure 1. PDUS scores of synovial blood flow. (a) 0, no flow signal in the synovium; (b) 1, single or few vessel signals; (c) 2, confluent vessel signals in less than half of the area of the synovium; and (d) 3, vessel signals in more than half of the area of the synovium. Arrows indicate synovium.

each joint, and the results were averaged. The following perfusion parameters were noted: shape parameters of the perfusion model, peak intensity (PT), area under the curve (AUC), and time-to-peak (TTP).

Ultrasound-guided synovial biopsy

Rabbits in the AIA group underwent ultrasound-guided biopsy after ultrasound imaging. The biopsy was targeted to the thickest synovial plane in the same knee recesses assessed by CEUS. For every joint capsule, a suitable coaxial outer needle was used in addition to an 18-gauge Magnum Biopsy Needle (Bard Medical, Covington, GA, USA). A longitudinal sonogram was used to follow the needle in real time and guide it to the appropriate predetermined biopsy site. Two independent samples were extracted from each knee at the hypertrophic synovium, including power Doppler-positive areas. Rabbits in the control group were sacrificed by injection of an overdose of sodium pentobarbital after CEUS examination. Two knee joints were harvested for

further histological investigations. All specimens were fixed in 10% formaldehyde for 24 hours.

Hematoxylin and eosin (H&E) staining and immunohistochemistry

The synovial samples were scored blindly by two experienced pathologists after routine H&E staining (Table 1), and samples with an intact or lower lining were included. Synovitis was scored according to the proliferation of the synovial lining cells, activation of the synovial stroma, and infiltration of inflammatory cells. Each of these three features was scored from 0 to 3, with a maximum total score of 9. Synovitis severity was graded from 0 to 3 according to the total score. Anti-CD31 antibody (Maxim, Fuzhou, China) immunostaining was carried out according to the labelled streptavidin biotin method (Dako LSAB kit, Glostrup, Denmark). The MVD in each joint was defined as the mean number of vessels in three microscopic fields (400×) with high MVD areas.

Table 1. Synovitis score.

	Pathological manifestation	Score
Hyperplasia enlargement	Lining cells form one layer, or absent	0
	Slight (2–3 cell layers), GCs very rare	1
	Moderate (4–5 cell layers), some GCs or LYMs	2
	Strong (>6 cell layers), GCs frequent	3
Inflammatory infiltration	Absent	0
	Slight	1
	Moderate	2
	Strong	3
Synovial stroma activation	Normal cellularity	0
	Slight	1
	Moderate	2
	Severe	3
Total score[a]		9

[a]Total score 0–1 for Grade 0, 2–3 for Grade 1, 4–6 for Grade 2, 7–9 for Grade 3.
Hyperplasia, hyperplasia of the synovial lining cell layer; GC, giant cell; LYM, lymphocyte.

Statistical analysis

Differences between the AIA and control groups were analyzed by Mann–Whitney two-sample tests and differences between the degree of vascularization on unenhanced PDUS and contrast-enhanced CEUS were evaluated by the Wilcoxon's signed-rank test. The association between ultrasound outcomes and MVD (CD31+ vessel count) or synovitis score were examined by Spearman's correlation analysis. $P < 0.05$ was considered significant. All statistical analyses were performed using IBM SPSS Statistics for Windows, version 15 (SPSS Inc., Chicago, IL, USA).

Results

Animals

Rabbits (n = 25) in the AIA group developed swollen knee joints with impaired functional ability. In contrast, no obvious abnormality was observed in the control rabbits (n = 5).

Results of ultrasound imaging

The ultrasound investigation was technically adequate for examination of the knee joints in the AIA and control groups. Neither unenhanced PDUS nor contrast-enhanced CEUS demonstrated any detectable intraarticular color-flow signals in the control group (10 knee joints). In the AIA group, there was no significant difference between the power Doppler frequency and amplitude modes in terms of the detection of intraarticular vascularization using unenhanced PDUS. Unenhanced PDUS detected synovial hyperplasia, manifested as an anechoic and hypoechoic area in the cavum articulate, and heterogeneous echogenicity in the posterior recess in the knee joint. The mean (± standard deviation) PDUS score was significantly higher in the AIA group (2.61 ± 0.78) compared with the control group (0.50 ± 0.53) ($P < 0.01$).

CEUS achieved uniform, subjectively optimal contrast enhancement with no substantial side effects of administration of the contrast agent. CEUS detected greater enhancement in the synovial membrane than in the surrounding tissues (Figure 2). The time-intensity curve indicated a fast-in/slow-out pattern of contrast enhancement, while the slope of the descending branch was relatively flatter (Figure 2). The CEUS
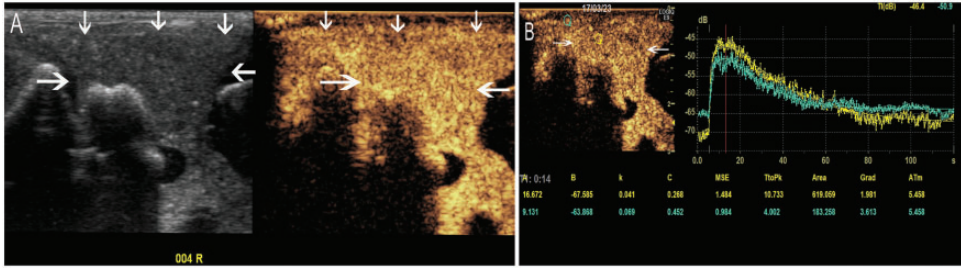
Figure 2. (a) Real-time grayscale contrast-enhanced ultrasound (CEUS) (real-time double side-by-side image display). Two-dimensional ultrasound on left showing synovial hyperplasia in the antigen-induced arthritis (AIA) group; CEUS on the right showing enhanced synovial membrane in the AIA group. (b) CEUS region of interest (yellow) was selected to obtain the time-intensity showing a fast-in/slow-out pattern, and quantitative parameters. Arrows indicate synovium.
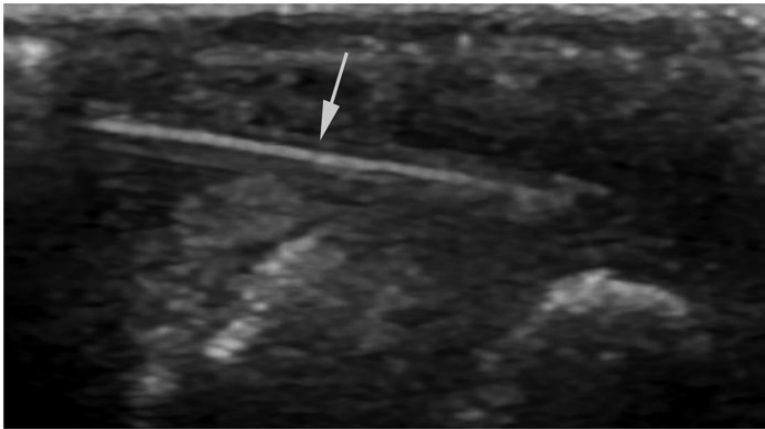

Figure 3. Ultrasound-guided synovial biopsy of a knee joint. The needle is clearly visible (arrow).

parameters in the AIA group were: PI: -52.65 ± 8.03 dB; AUC: 568.35 ± 315.68; and TTP: 9.18 ± 6.03 seconds.

Histologic findings

Of the 25 rabbits in the AIA group, ultrasound-guided synovial biopsies were obtained successfully in 23 (46 joints; 92%) (Figure 3). No synovial inflammation was observed in the control group, including hyperplasia of synovial lining cells and stroma, or infiltration of inflammatory cells in the lower lining. In contrast, histological findings revealed increased numbers of synovial lining cells, infiltration of inflammatory cells in the sub-synovial lining, fibrous degeneration with interstitial edema, and cellulose exudation in the AIA group. Most inflammatory cells were lymphocytes, monocytes, and plasma cells, and infiltration of eosinophils and neutrophils was noted. Obvious vascular proliferation was seen in the synovium, especially in rabbits with severe synovitis (Figure 4). The synovitis score was significantly higher in the AIA group (46 samples; 5.12 ± 3.68) compared with control group
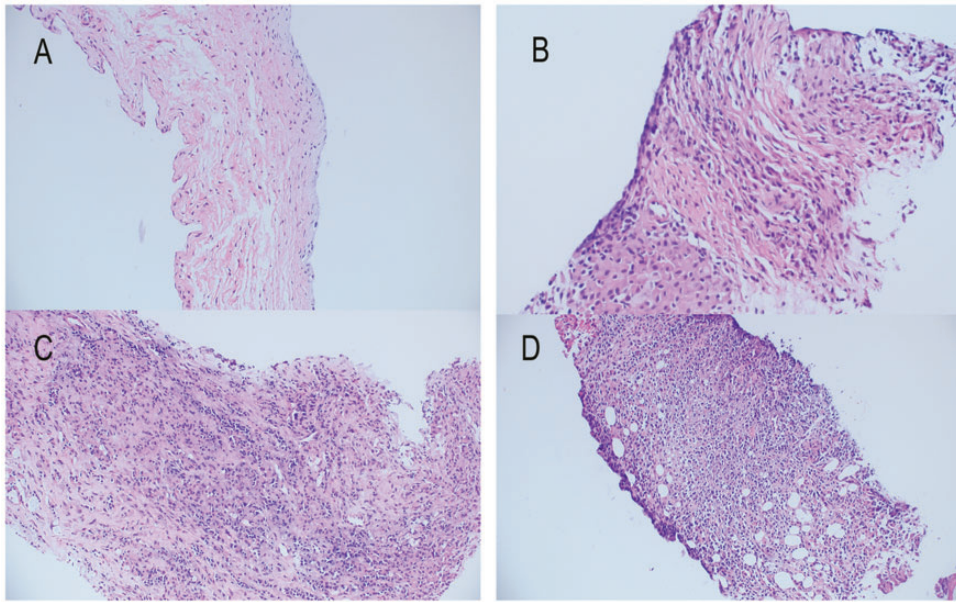
Figure 4. Synovitis scores. Histologic aspects of the antigen-induced arthritis group, showing enlarged cell layer lining, cellular density of the synovial stroma, and the presence of inflammatory infiltrate (hematoxylin–eosin, original magnification ×200). The severity of synovitis increases from a to d (score 0 to 3).

Table 2. Contrast-enhanced ultrasound parameters according to synovitis score in the antigen-induced arthritis group.

	Synovitis score (n)			
	0 (2)	1 (7)	2 (23)	3 (14)
Peak intensity	−63.67 ± 4.59	−61.73 ± 7.95*	−56.99 ± 8.15*	−51.33 ± 7.89*
Time-to-peak	9.83 ± 3.51	10.13 ± 4.07	10.47 ± 5.95	10.07 ± 5.83
AUC	214.52 ± 56.36	589.95 ± 335.12	653.36 ± 492.79	713.45 ± 487.93
PDUS score	0	1.50 ± 0.50*	2.31 ± 0.62*	2.83 ± 0.54*

Data presented as mean ± standard deviation where applicable.
*$P<0.05$ for 1 compared with 2, or 2 compared with 3.

(10 samples; 1.21 ± 0.53) ($P<0.05$), and two, seven, 23, and 14 samples in the AIA group were graded as 0, 1, 2, and 3, respectively (Table 2). The MVD, indicated by CD31+ vessel count, was significantly higher in the AIA group (46 samples; 89 ± 38) compared with the control group (10 samples; 41 ± 15) ($P<0.05$) (Figure 5).

Associations between ultrasound findings and MVD and synovitis score

CEUS findings showed a better correlation with MVD determined by CD31+ than did PDUS findings in the AIA group. PI was significantly correlated with MVD via CD31+ ($r=0.436$, $P<0.01$). The PDUS
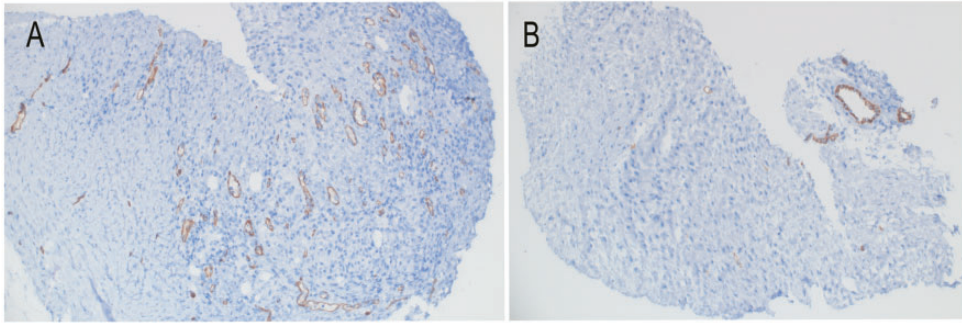
Figure 5. Immunohistochemical staining of CD31 (200×). (a) Rich vessels in synovial and subsynovial layers in the antigen-induced arthritis group (in brown). (b) Few vessels in synovial and subsynovial layers in the control group.

score was also significantly correlated with MVD via CD31+ ($r = 0.328$, $P < 0.05$). However, similar results were not found for TTP and AUC.

Similarly, CEUS findings also correlated better with synovitis score than did PDUS findings in the AIA group. Among all the CEUS parameters, PI scored the highest and was significantly correlated with synovitis score ($r = 0.578$, $P < 0.01$). The PDUS score was also significantly correlated with synovitis score ($r = 0.354$, $P < 0.05$).

Discussion

Our preliminary data demonstrated that CEUS perfusion kinetics had a better association with the histopathological quantitative and morphologic estimation of synovial hypervascularity and hyperplasia in experimental rheumatoid arthritis than PDUS findings. The vasculature is highly organized and well-defined in normal joints, but vascular turnover is increased in joints with arthritis, leading to a compromised ability to regulate blood flow.[42] As a direct proxy of histopathological change at a single-joint level, microvascular perfusion kinetics are crucial to the development and evaluation of imaging techniques.[43–45]

The current results suggest that CEUS quantitatively reflects neoangiogenesis and synovitis better than PDUS in experimental RA. The early diagnosis of RA and the differentiation between inactive and active inflammatory synovial membranes and joints are critical issues for developing a T2T strategy.[46,47] Although conventional radiology is the most commonly used imaging in RA, it has limited value for characterizing soft tissues.[48] Magnetic resonance imaging has an excellent ability to examine the soft tissue, but has limited availability and is cost-ineffective.[48–51] Advancements in ultrasound, including increased resolution of the ultrasonographic images and higher frequencies or smaller probes for transducers, play an important part in the diagnosis of early RA.[52,53] PDUS detected the difference in vascularization between inactive versus moderately active and active RA, but failed to demonstrate any difference between moderately active and active joints.[19] Given that abnormal synovial vascularity is evident with the onset of joint inflammation, estimating the level of joint inflammation by sonographic synovial vascularity is useful for achieving a T2T strategy.[10]

Our results clearly demonstrate that CEUS is superior to PDUS for detecting intraarticular vascularization. Recent studies revealed inconsistent findings regarding

the assessment of hypervascularization with PDUS.[11–14] In agreement with a previous study that revealed positive correlations between MVD and pathological scores, and expression of vascular endothelial growth factor and hypoxia-inducible factor-1α in the synovium in collagen-induced arthritis,[54] our results showed a correlation between peak intensity in perfusion parameters on CEUS and MVD revealed by CD31 staining.

CD31 is expressed in both undifferentiated and differentiated endothelial cells,[55] and may thus reflect the complete profile of synovial neovascularization. PDUS only detected blood flow signals in vessels >100 μm,[34] while CEUS with SonoVue detected synovial vessels <50 μm.[34] Moreover, ultrasound contrast agents are less likely to leak into the synovial fluid than magnetic resonance imaging contrast agents, thus providing a more accurate reflection of synovial and vascular changes in the joint.[56] CEUS thus increases the possibility of identifying patients with latent but progressive RA based on the good association between CEUS findings and hypervascularization.

In addition to revealing the progression of vessel formation, CEUS presented different enhancement patterns at different disease stages in a cancer model, and importantly identified angiogenesis before the change in color Doppler.[57] Neovascularization during the transitory pre-vascular highly inflammatory stage in RA mainly consists of small immature and dilated vessels and the vascular muscular layer is not complete.[9] Besides, CEUS provides valuable information about the spatial distribution of blood flow and vascular volume compares with a validated contrast-enhanced CT method.[58]

Our findings also demonstrated that CEUS detected synovitis as peak intensity, as an index reflecting synovial blood volume, which correlated with synovitis score better than did PDUS scores.

Increased vessel permeability resulting from synovial hypervascularization induced the infiltration of inflammatory cells and the production of inflammatory mediators, finally imitating and aggravating synovitis.[59] CEUS quantifies the degree and extent of synovial inflammation and disease activity, which is crucial for the diagnosis and follow-up of patients with RA, particularly in early-stage disease.

The CEUS method adopted in this study was well tolerated with no important clinical side effects. This technique might thus be translated into the routine clinical examination of RA patients, to allow the early acquisition of information on synovial angiogenesis and hyperplasia, to help confirm disease progression or remission and guide the therapeutic strategy.

This study was limited by it being a cross-sectional study and the results were only examined after 8 weeks. Further, longitudinal studies are therefore planned to explore the efficacy of early detection of RA.

Conclusion

We conclude that the administration of a contrast agent can improve the detection of synovial hypervascularity and hyperplasia compared with unenhanced ultrasound. Furthermore, CEUS will allow the assessment of enhancement kinetics to improve the detection of disease activity.

Declaration of conflicting interest

The authors declare that there is no conflict of interest.

Ethics approval

The study protocol was approved by the Animal Ethics and Welfare Committee of Fujian Medical University (reference number of SYXK [min] 2016–0008).

Funding

ORCID iD

Guorong Lv https://orcid.org/0000-0003-3123-1138

References

1. McInnes IB and Schett G. The pathogenesis of rheumatoid arthritis. *N Engl J Med* 2011; 365: 2205–2219.
2. Smolen JS, Aletaha D and McInnes IB. Rheumatoid arthritis. *Lancet* 2016; 388: 2023–2038.
3. Burmester GR and Pope JE. Novel treatment strategies in rheumatoid arthritis. *Lancet* 2017; 389: 2338–2348.
4. Zvaifler NJ and Firestein GS. Pannus and pannocytes. Alternative models of joint destruction in rheumatoid arthritis. *Arthritis Rheum* 1994; 37: 783–789.
5. FitzGerald O and Bresnihan B. Synovial membrane cellularity and vascularity. *Ann Rheum Dis* 1995; 54: 511–515.
6. FitzGerald O, Soden M, Yanni G, et al. Morphometric analysis of blood vessels in synovial membranes obtained from clinically affected and unaffected knee joints of patients with rheumatoid arthritis. *Ann Rheum Dis* 1991; 50: 792–796.
7. Bodolay E, Koch AE, Kim J, et al. Angiogenesis and chemokines in rheumatoid arthritis and other systemic inflammatory rheumatic diseases. *J Cell Mol Med* 2002; 6: 357–376.
8. Polzer K, Baeten D, Soleiman A, et al. Tumour necrosis factor blockade increases lymphangiogenesis in murine and human arthritic joints. *Ann Rheum Dis* 2008; 67: 1610–1616.
9. Leblond A, Allanore Y and Avouac J. Targeting synovial neoangiogenesis in rheumatoid arthritis. *Autoimmun Rev* 2017; 16: 594–601.
10. Fukae J, Tanimura K, Atsumi T, et al. Sonographic synovial vascularity of synovitis in rheumatoid arthritis. *Rheumatology (Oxford)* 2014; 53: 586–591.
11. Andersen M, Ellegaard K, Hebsgaard JB, et al. Ultrasound colour Doppler is associated with synovial pathology in biopsies from hand joints in rheumatoid arthritis patients: a cross-sectional study. *Ann Rheum Dis* 2014; 73: 678–683.
12. Takase K, Ohno S, Takeno M, et al. Simultaneous evaluation of long-lasting knee synovitis in patients undergoing arthroplasty by power Doppler ultrasonography and contrast-enhanced MRI in comparison with histopathology. *Clin Exp Rheumatol* 2012; 30: 85–92.
13. Koski JM, Saarakkala S, Helle M, et al. Power Doppler ultrasonography and synovitis: correlating ultrasound imaging with histopathological findings and evaluating the performance of ultrasound equipments. *Ann Rheum Dis* 2006; 65: 1590–1595.
14. Walther M, Harms H, Krenn V, et al. Correlation of power Doppler sonography with vascularity of the synovial tissue of the knee joint in patients with osteoarthritis and rheumatoid arthritis. *Arthritis Rheum* 2001; 44: 331–338.
15. Olivieri I, Barozzi L, Favaro L, et al. Dactylitis in patients with seronegative spondylarthropathy. Assessment by ultrasonography and magnetic resonance imaging. *Arthritis Rheum* 1996; 39: 1524–1528.
16. Grassi W, Tittarelli E, Pirani O, et al. Ultrasound examination of metacarpophalangeal joints in rheumatoid arthritis. *Scand J Rheumatol* 1993; 22: 243–247.
17. Newman JS, Laing TJ, McCarthy CJ, et al. Power Doppler sonography of synovitis: assessment of therapeutic response–preliminary observations. *Radiology* 1996; 198: 582–584.
18. Schmidt WA, Völker L, Zacher J, et al. Colour Doppler ultrasonography to detect pannus in knee joint synovitis. *Clin Exp Rheumatol* 2000; 18: 439–444.
19. Hau M, Schultz H, Tony HP, et al. Evaluation of pannus and vascularization of the metacarpophalangeal and proximal

interphalangeal joints in rheumatoid arthritis by high-resolution ultrasound (multidimensional linear array). *Arthritis Rheum* 1999; 42: 2303–2308.

20. Rednic N, Tamas MM and Rednic S. Contrast-enhanced ultrasonography in inflammatory arthritis. *Med Ultrason* 2011; 13: 220–227.

21. Goldberg BB, Liu JB and Forsberg F. Ultrasound contrast agents: a review. *Ultrasound Med Biol* 1994; 20: 319–333.

22. Klauser A, Frauscher F, Schirmer M, et al. The value of contrast-enhanced color Doppler ultrasound in the detection of vascularization of finger joints in patients with rheumatoid arthritis. *Arthritis Rheum* 2002; 46: 647–653.

23. Kleffel T, Demharter J, Wohlgemuth W, et al. [Comparison of contrast-enhanced low mechanical index (Low MI) sonography and unenhanced B-mode sonography for the differentiation between synovitis and joint effusion in patients with rheumatoid arthritis]. *Rofo* 2005; 177: 835–841.

24. Qvistgaard E, Røgind H, Torp-Pedersen S, et al. Quantitative ultrasonography in rheumatoid arthritis: evaluation of inflammation by Doppler technique. *Ann Rheum Dis* 2001; 60: 690–693.

25. Stramare R, Raffeiner B, Ciprian L, et al. Evaluation of finger joint synovial vascularity in patients with rheumatoid arthritis using contrast-enhanced ultrasound with water immersion and a stabilized probe. *J Clin Ultrasound* 2012; 40: 147–154.

26. Fiocco U, Stramare R, Coran A, et al. Vascular perfusion kinetics by contrast-enhanced ultrasound are related to synovial microvascularity in the joints of psoriatic arthritis. *Clin Rheumatol* 2015; 34: 1903–1912.

27. Fiocco U, Stramare R, Martini V, et al. Quantitative imaging by pixel-based contrast-enhanced ultrasound reveals a linear relationship between synovial vascular perfusion and the recruitment of pathogenic IL-17A-F(+)IL-23(+) CD161(+) CD4(+) T helper cells in psoriatic arthritis joints. *Clin Rheumatol* 2017; 36: 391–399.

28. Qiu L, Jiang Y, Zhang L, et al. Ablation of synovial pannus using microbubble-mediated ultrasonic cavitation in antigen-induced arthritis in rabbits. *Rheumatol Int* 2012; 32: 3813–3821.

29. Chen S, Zheng Q, Liu H, et al. Sonography is superior to serum-based biomarkers for measuring disease status in experimental rheumatoid arthritis. *J Ultrasound Med* 2016; 35: 2223–2230.

30. Asahara T, Murohara T, Sullivan A, et al. Isolation of putative progenitor endothelial cells for angiogenesis. *Science* 1997; 275: 964–967.

31. Poblet E, Gonzalez-Palacios F and Jimenez FJ. Different immunoreactivity of endothelial markers in well and poorly differentiated areas of angiosarcomas. *Virchows Arch* 1996; 428: 217–221.

32. Xing J, He W, Ding YW, et al. Correlation between contrast-enhanced ultrasound and microvessel density via CD31 and CD34 in a rabbit VX2 lung peripheral tumor model. *Med Ultrason* 2018; 1: 37–42.

33. Zhou Q, Jiang J, Shang X, et al. Correlation of contrast-enhanced ultrasonographic features with microvessel density in papillary thyroid carcinomas. *Asian Pac J Cancer Prev* 2014; 15: 7449–7452.

34. Zhuo J, Fu W and Liu S. Correlation of contrast-enhanced ultrasound with two distinct types of blood vessels for the assessment of angiogenesis in Lewis lung carcinoma. *Ultraschall Med* 2014; 35: 468–472.

35. Wang Y, Yan K, Fan Z, et al. Contrast-enhanced ultrasonography of pancreatic carcinoma: correlation with pathologic findings. *Ultrasound Med Biol* 2016; 42: 891–898.

36. Atkinson EG, Dinning WJ, Kasp E, et al. Precipitation of experimental autoallergic uveoretinitis by cyclosporin A withdrawal: an experimental model of uveitis relapse. *Clin Exp Immunol* 1989; 78: 108–114.

37. Glynn LE. Experimental model of rheumatoid arthritis. *J Belge Rhumatol Med Phys* 1967; 22: 201–203.

38. Kilkenny C, Browne WJ, Cuthill IC, et al. Improving bioscience research reporting: the ARRIVE guidelines for reporting animal research. *PLoS Biol* 2010; 8: e1000412.

39. Szkudlarek M, Court-Payen M, Jacobsen S, et al. Interobserver agreement in ultrasonography of the finger and toe joints in

rheumatoid arthritis. *Arthritis Rheum* 2010; 48: 955–962.

40. Chakr RM, Mendonça JA, Brenol CV, et al. Assessing rheumatoid arthritis disease activity with ultrasound. *Clin Rheumatol* 2013; 32: 1249–1254.

41. Alivernini S, Tolusso B, Petricca L, et al. Synovial predictors of differentiation to definite arthritis in patients with seronegative undifferentiated peripheral inflammatory arthritis: microRNA signature, histological, and ultrasound features. *Front Med (Lausanne)* 2018; 5: 186.

42. Haywood L and Walsh DA. Vasculature of the normal and arthritic synovial joint. *Histol Histopathol* 2001; 16: 277–284.

43. Kurikawa Y and Ahlqvist J. Joint fluid hydrostatic pressures that empty synovial capillaries of red cells have a wide range and correlate with pressures emptying arterioles. *J Rheumatol* 1998; 25: 1364–1368.

44. Levick JR. Hypoxia and acidosis in chronic inflammatory arthritis; relation to vascular supply and dynamic effusion pressure. *J Rheumatol* 1990; 17: 579–582.

45. Jain RK. Determinants of tumor blood flow: a review. *Cancer Res* 1988; 48: 2641–2658.

46. Combe B, Landewe R, Daien CI, et al. 2016 update of the EULAR recommendations for the management of early arthritis. *Ann Rheum Dis* 2017; 76: 948–959.

47. Smolen JS, Breedveld FC, Burmester GR, et al. Treating rheumatoid arthritis to target: 2014 update of the recommendations of an international task force. *Ann Rheum Dis* 2016; 75: 3–15.

48. Ostergaard M, Gideon P, Sørensen K, et al. Scoring of synovial membrane hypertrophy and bone erosions by MR imaging in clinically active and inactive rheumatoid arthritis of the wrist. *Scand J Rheumatol* 1995; 24: 212–218.

49. Ostergaard M, Stoltenberg M, Løvgreen-Nielsen P, et al. Quantification of synovitis by MRI: correlation between dynamic and static gadolinium-enhanced magnetic resonance imaging and microscopic and macroscopic signs of synovial inflammation. *Magn Reson Imaging* 1998; 16: 743–754.

50. Gaffney K, Cookson J, Blades S, et al. Quantitative assessment of the rheumatoid synovial microvascular bed by gadolinium-DTPA enhanced magnetic resonance imaging. *Ann Rheum Dis* 1998; 57: 152–157.

51. Waterton JC, Rajanayagam V, Ross BD, et al. Magnetic resonance methods for measurement of disease progression in rheumatoid arthritis. *Magn Reson Imaging* 1993; 11: 1033–1038.

52. Schmidt WA. Value of sonography in diagnosis of rheumatoid arthritis. *Lancet* 2001; 357: 1056–1057.

53. Bhasin S and Cheung PP. The role of power Doppler ultrasonography as disease activity marker in rheumatoid arthritis. *Dis Markers* 2015; 2015: 325909.

54. Xu J, Feng Z, Chen S, et al. Taxol alleviates collagen-induced arthritis in mice by inhibiting the formation of microvessels. *Clin Rheumatol* 2019; 38: 19–27.

55. Qian CN, Huang D, Wondergem B, et al. Complexity of tumor vasculature in clear cell renal cell carcinoma. *Cancer* 2010; 115: 2282–2289.

56. Gibbon WW and Wakefield RJ. Ultrasound in inflammatory disease. *Radiol Clin North Am* 1999; 37: 633–651.

57. Wang M, Feng HL, Liu YQ, et al. Angiogenesis research in mouse mammary cancer based on contrast-enhanced ultrasonography: exploratory study. *Acad Radiol* 2018; 25: 889–897.

58. Ferrara KW. Contrast-enhanced computed tomography and ultrasound for the evaluation of tumor blood flow. *Invest Radiol* 2005; 40: 134–147.

59. Konisti S, Kiriakidis S and Paleolog EM. *Angiogenesis in rheumatoid arthritis.* Vienna: Springer, 2013.